ELSEVIER

International Journal of Solids and Structures 41 (2004) 145–157

INTERNATIONAL JOURNAL OF SOLIDS and STRUCTURES

www.elsevier.com/locate/ijsolstr

Electrical fracture toughness for a conducting crack in ferroelectric ceramics

H.K. Beom *, S.K. Youn

Department of Mechanical Engineering, Korea Advanced Institute of Science and Technology, 371-1 Kusong-dong, Yusung-gu, Taejon 305-701, South Korea

Received 26 March 2003

Abstract

Conducting cracks in ferroelectric ceramics under purely electrical loading are analyzed to investigate the effects of electric fields on fracture behavior. The asymptotic problem of conducting cracks in a mono-domain ferroelectric material as well as in a poly-domain ferroelectric material is considered and the relation between the crack tip stress intensity factor and the applied intensity factor of electric field under small scale conditions is investigated. In order to evaluate the crack tip stress intensity factors due to the domain switching, the shape of the domain switching zone attending the crack tip must be determined. The evaluation of the shape is carried out based on the nonlinear domain switching model. It is shown that the switching zone boundary and the crack tip stress intensity factors due to the switching depend strongly on the angle of the polarization vector and the ratio of the coercive electric field to the yield electric field. The electrical fracture toughness of unpoled poly-domain ferroelectrics is examined. Employing a Reuss type approximation, the crack tip stress intensity factors for an unpoled poly-domain material are obtained. The ratio of the critical electrical energy release rate to the critical mechanical energy release rate is obtained.

Keywords: Asymptotic analysis; Crack; Ferroelectrics; Fracture

1. Introduction

Ferroelectric ceramics have recently attracted much attention for engineering applications in capacitors, sensors, actuators and nonvolatile memories. It is of great importance to understand fracture behavior of ferroelectric ceramics since ferroelectric ceramics are brittle. Crack growth in a ferroelectric material under electric or mechanical loading has recently gained importance, due to its potential application in various kinds of reliability problems. Many efforts have focused on studying the effects of an electrical field on the crack growth in a ferroelectric material. Extensive studies have been carried out on the dielectric breakdown associated with growth of conducting cracks. Heyer et al. (1998) used four point bending tests to investigate the growth of conducting cracks parallel to the poling axis in poled PZT-PIC 151 under combined

* Corresponding author. Tel.: +82-42-869-3074; fax: +82-42-869-3095.
E-mail addresses: s_bhk@kaist.ac.kr (H.K. Beom), skyoun@sorak.kaist.ac.kr (S.K. Youn).

0020-7683/$ - see front matter © 2003 Elsevier Ltd. All rights reserved.
doi:10.1016/j.ijsolstr.2003.07.005

mechanical and electrical loading. They observed that the apparent fracture toughness is increased under a positive electric field with the same direction of the polarization, while a low negative electric field with the direction opposite to the polarization reduces the apparent toughness. At low applied electric fields, their experimental result of fracture curve was also found to be in good agreement with that predicted by a fracture criterion based on the total energy release rate. However, their result showed that a positive electric field as well as a negative electric field impede crack propagation when the applied electric loads are sufficiently large. This implies that fracture of the piezoelectric material may not be caused under purely electric loading. Fu et al. (2000) experimentally studied fracture behavior of conducting cracks in a poled PZT-4 subjected to purely electrical loading. They observed that growth of the conducting crack occurs under purely electric loading, and the electric fracture toughness in terms of the energy release rate is much higher than the mechanical fracture toughness. Subsequently Wang and Zhang (2001) performed conventional fracture tests to investigate electric field effects on conducting crack growth in a depoled PZT-4 ceramic without piezoelectricity under purely electrical loading. They obtained the result consistent with that of Fu et al. (2000). As seen in the previous experimental works, conducting crack extension under purely electric loading will depends on individual ferroelectric material.

Several theoretical models have been proposed to evaluate the effect of electric field on fracture toughness of ferroelectric ceramics. The linear theory predicts that the electric fracture toughness and the mechanical fracture toughness in terms of the energy release rate are the same (Suo, 1993), which disagrees with the experimental observations. Ru and Mao (1999) employed the model of strip saturation near the conducting crack tip to examine the effect of the electrical nonlinearity on fracture behavior. Their result showed that purely electric loading parallel to the poling direction does not induce any stress intensity factor for a conducting crack parallel to the poling direction. This result, however, does not give a theoretical explanation for the experimental observation of Heyer et al. (1998). Rajapakse and Zeng (2001) rigorously evaluated fracture toughness variation in anisotropic ferroelectrics with electromechanical coupling based on the linear domain switching model. While their model predicted the result consistent with the experimental observation of Heyer et al. (1998), their results could not provide a theoretical interpretation interpretation for the experimental observation in Fu et al. (2000) and Wang and Zhang (2001). Han et al. evaluated the crack tip intensity employed asymptotic analysis based on linear model. The models mentioned above thus do not give theoretical explanations for the various experimental observations on fracture behavior of ferroelectric materials. Recently, Beom and Atluri (2003) performed the insulate crack problem considered nonlinearity of ferroelectrics.

It is the purpose of this study to investigate effect of electric fields on fracture behavior of ferroelectric ceramics subjected to purely electric loading. In order to derive the relation between the crack tip stress intensity factor and the applied intensity factor of electric field under small scale conditions, the asymptotic problem of a conducting crack in a ferroelectric material is considered. For the evaluation of the crack tip intensity factor due to the domain switching, the shape of the domain switching zone attending the crack tip is estimated based on the nonlinear domain switching model. It is shown that the switching zone boundary and the crack tip stress intensity factors due to the switching depend strongly on the angle of the polarization vector and the ratio of the coercive electric field to the yield electric field. The electrical fracture toughness of unpoled poly-domain ferroelectrics is examined. Employing a Reuss type approximation, the crack tip stress intensity factor for an unpoled poly-domain ferroelectric material is obtained.

2. Ferroelectric ceramics

Ceramic materials showing ferroelectric behavior possess domains with uniform polarization. Ferroelectric switching occurs when sufficiently large external loads such as electric field and stress are applied. The phenomenon characterizes a feature of ferroelectrics. Ferroelectric materials are also known to have

strongly electric nonlinearities at high field strength. When an applied electric field exceeds the yield electric field, the electric displacement of a ferroelectric material approaches finite limit, referred to as electric saturation. Although there has been much progress in a constitutive law for nonlinear ferroelectric ceramics, much attention has been still devoted to constitutive models of ferroelectric ceramics for domain switching and electric saturation (Hwang et al., 1995; Huber et al., 1999; Kamlah and Tsakmakis, 1999; Sze and Pan, 2001).

In order to investigate fracture behavior of ferroelectrics under electric loading, a simple constitutive model for the ferroelectric ceramics is here introduced. The ferroelectric material is assumed to have perfect polarization saturation (Beom and Atluri, 2003).

This idealization is useful in carrying out detailed analysis of fracture behavior. An idealized model of material behavior of typical ferroelectric ceramics is illustrated for the electric displacement versus electric field in Fig. 1. The ferroelectric material has the coercive electric field E_c, the yield electric field E_0 and the spontaneous polarization P_s.

Consider a ferroelectric material with a uniformly poled domain. The initial polarization vector forms an angle ϕ with x_1-axis. As external loads such as electric field and stress attain sufficiently large values, 90° or 180° domain switchings can be induced. According to a proposal by Hwang et al. (1995), domain switching occurs when the sum of the electrical and the mechanical work exceeds a critical value, that is

$$\sigma_{ij}\Delta\gamma_{ij} + E_i\Delta P_i \geqslant 2P_sE_c. \tag{1}$$

Here σ_{ij} and E_i are the stress tensor and the electric field vector, respectively. $\Delta\gamma_{ij}$ and ΔP_i denote the switching strain tensor and polarization switch vector, respectively. The polarization switch vector due to 90° domain switching and the switching strain tensor associated with the 90° domain switching are given as (Yang and Zhu, 1998):

$$\begin{aligned} \Delta P_i &= \sqrt{2}P_s\begin{Bmatrix} \cos\left(\phi \pm \tfrac{3}{4}\pi\right) \\ \sin\left(\phi \pm \tfrac{3}{4}\pi\right) \end{Bmatrix}, \\ \Delta\gamma_{ij} &= \gamma_s\begin{bmatrix} -\cos 2\phi & -\sin 2\phi \\ -\sin 2\phi & \cos 2\phi \end{bmatrix}, \end{aligned} \tag{2}$$

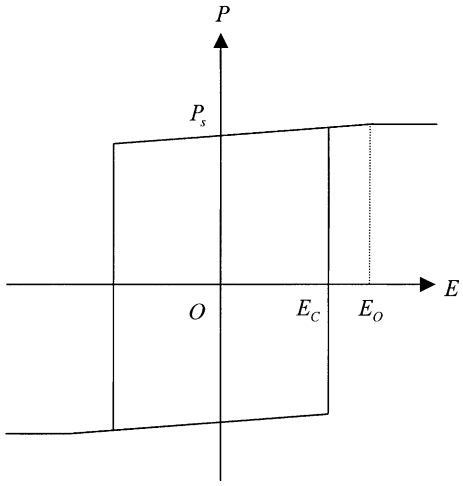

Fig. 1. Idealized hysteresis loop of electric polarization with perfect saturation.

where γ_s is the spontaneous strain associated with 90° domain switching, and the values of $-\frac{3}{4}\pi$ and $+\frac{3}{4}\pi$ in (2) indicate the quantities for clockwise and counterclockwise 90° switchings, respectively. For 180° domain switching, the polarization switch vector and switching strain tensor are given, respectively as

$$\begin{aligned} \Delta P_i &= -2P_s \begin{Bmatrix} \cos\phi \\ \sin\phi \end{Bmatrix}, \\ \Delta\gamma_{ij} &= 0. \end{aligned} \tag{3}$$

The mechanical load satisfying the switching criterion (1) induces only 90° domain switching since no switching strains are induced due to the 180° switching, whereas the electrical loading can generate 90° or 180° domain switchings.

3. Crack tip fields

Consider a conducting crack in a mono-domain ferroelectric ceramic with a polarization vector forming an angle ϕ with x_1-axis under purely electrical loading. The crack surfaces are traction-free and electrically conductive. Assume that the sizes of the electrical nonlinear zone and the switching zone around the crack tip are sufficiently small compared to the length of the crack in order to investigate the effect of the electric field on fracture behavior under the small scale conditions. We consider thus the asymptotic problem of a semi-infinite crack in a ferroelectric ceramic under purely electrical loading as shown in Fig. 2. In this paper, the material is assumed to be isotropic. The remote fields in the asymptotic problem under the small scale conditions are prescribed to be the near-tip fields for the crack in the linear material. The electric field at infinity is written as

$$E_i = \frac{K_E^\infty}{\sqrt{2\pi r}} \widetilde{E}_i(\theta). \tag{4}$$

Here K_E^∞ denotes the applied intensity factor of the electric field. We are only concerned with the case of $K_E^\infty > 0$ in this paper. (r, θ) is the cylindrical coordinates centered at the tip of the crack as shown in Fig. 2. $\widetilde{E}_i(\theta)$ is the universal distribution functions of electric field for the conducting crack in the linear material. The solution of the electric field for the asymptotic problem can be found in Beom (1999). The shape of the

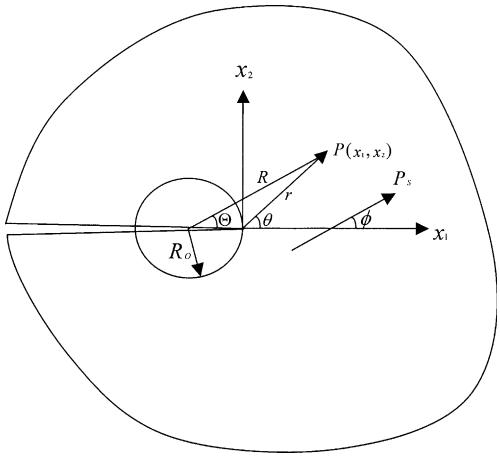

Fig. 2. An asymptotic problem of crack in a ferroelectric material.

electrical saturation zone boundary is a circle of radius R_0 centered on the x_1-axis at $x_1 = -R_0$. Here R_0 is given by

$$R_0 = \frac{1}{2\pi}\left(\frac{K_{\mathrm{E}}^{\infty}}{E_0}\right)^2. \tag{5}$$

The electric fields inside the electrical nonlinear zone ($R < R_0$) where the ceramic is the perfect saturation material can be written as

$$E_r = 0,$$
$$E_\theta = \begin{cases} -\frac{2E_0R_0}{r}\cos\theta & -\pi < \theta < -\frac{1}{2}\pi, \\ \frac{2E_0R_0}{r}\cos\theta & \frac{1}{2}\pi < \theta < \pi. \end{cases} \tag{6}$$

A convenient coordinate system which allows a compact form of the electric field outside the electrical nonlinear zone is the cylindrical coordinates (R, Θ) with the origin located at the point $x_1 = -R_0$ and $x_2 = 0$ as shown in Fig. 2. The solution of the electric fields outside the electrical nonlinear zone ($R > R_0$) where the material is linear dielectric is known as

$$E_R = \frac{K_{\mathrm{E}}^{\infty}}{\sqrt{2\pi R}}\cos\frac{1}{2}\Theta,$$
$$E_\Theta = -\frac{K_{\mathrm{E}}^{\infty}}{\sqrt{2\pi R}}\sin\frac{1}{2}\Theta. \tag{7}$$

In the vicinity of the crack tip, the material is still linearly elastic whereas the material shows the electrical nonlinearity. The stress field at a point close to the crack tip is thus expressed as

$$\sigma_{ij} = \frac{K_{\mathrm{I}}^{\mathrm{tip}}}{\sqrt{2\pi r}}\tilde{\sigma}_{ij}^{\mathrm{I}}(\theta) + \frac{K_{\mathrm{II}}^{\mathrm{tip}}}{\sqrt{2\pi r}}\tilde{\sigma}_{ij}^{\mathrm{II}}(\theta) \quad \text{as } r \to 0, \tag{8}$$

where $K_{\mathrm{I}}^{\mathrm{tip}}$ and $K_{\mathrm{II}}^{\mathrm{tip}}$ represent the crack tip stress intensity factors of the Mode I and Mode II, respectively. $\tilde{\sigma}_{ij}^{\mathrm{I}}(\theta)$ and $\tilde{\sigma}_{ij}^{\mathrm{II}}(\theta)$ are the universal distribution functions of stress for the Mode I and Mode II, respectively. The crack tip stress intensity factors are induced by the switching strains, which will be exactly determined later.

4. Domain switching zone

In order to derive the relation between the crack tip stress intensity factor and the applied intensity factor of electric field under small scale conditions, we consider the asymptotic problem of a semi-infinite stationary crack lying along the negative x_1-axis. According to the electric field solution discussed in the previous section, the electric field is intensified around the tip of the crack. There is a region around the tip of a crack where polarization switching occurs, which is known as the domain switching zone. We first estimate the shape of the domain switching zone attending the crack tip in order to evaluate the crack tip stress intensity factor due to the domain switching. Mathematical difficulties prevent an exact solution of the domain switching zone since the switching strain results in stress redistribution and modifies the size and the shape of the domain switching zone. The analytical detail of the exact switching zone determination is somewhat complicated. However, the change of the stress distribution due to the switching strains around the switching zone boundary may be small since additional stresses due to the domain switching are confined to a small zone around the crack tip. Thus, the influence of stress redistribution on the crack tip stress intensity factor is negligible as mentioned in elasticity problem by McMeeking and Evans (1982) and

Budiansky et al. (1983). Neglecting the zone shape changes due to the stress induced by the switching, a first estimate of the switching zone boundary attending the crack tip can be obtained by using the electric fields (7) and (8). Substitution of the electric fields (7) and (8) into the switching criterion (1) leads to the following dimensionless form of an expression for the switching zone boundary:

$$r/R_c = \tilde{r}(\theta; E_c/E_0, \phi), \tag{9}$$

where R_c is given as

$$R_c = \frac{1}{2\pi}\left(\frac{K_E^\infty}{E_c}\right)^2. \tag{10}$$

The length parameter R_c is employed as a reference length scale to normalize the coordinates. Substituting the relations (2), (7) and (8) into the domain switching criterion (1), we obtain expressions for the 90° switching zone boundaries as a function of θ and Θ for inside and outside the electrical nonlinear zone, respectively:

$$\begin{aligned} \frac{r}{R_c} &= \begin{cases} -\sqrt{2}\frac{E_c}{E_0}\cos\theta\sin\left(-\theta+\phi\pm\frac{3}{4}\pi\right) & -\pi<\theta<-\frac{1}{2}\pi \\ \sqrt{2}\frac{E_c}{E_0}\cos\theta\sin\left(-\theta+\phi\pm\frac{3}{4}\pi\right) & \frac{1}{2}\pi<\theta<\pi \end{cases} \quad \text{for } R>R_0, \\ \sqrt{\frac{R}{R_c}} &= \frac{1}{\sqrt{2}}\frac{K_E^\infty}{|K_E^\infty|}\cos\left\{\frac{1}{2}\Theta-\left(\phi\pm\frac{3}{4}\pi\right)\right\} \quad \text{for } R>R_0. \end{aligned} \tag{11}$$

Here $+\frac{3}{4}\pi$ and $-\frac{3}{4}\pi$ are selected so as to give higher values of the switching zone boundaries r and R. In a similar manner, it can be shown that the expressions for the 180° switching zone boundaries are given as:

$$\begin{aligned} \frac{r}{R_c} &= \begin{cases} -2\frac{E_c}{E_0}\cos\theta\sin(\theta-\phi) & -\pi<\theta<-\frac{1}{2}\pi \\ 2\frac{E_c}{E_0}\cos\theta\sin(\theta-\phi) & \frac{1}{2}\pi<\theta<\pi \end{cases} \quad \text{for } R<R_0, \\ \sqrt{\frac{R}{R_c}} &= -\frac{1}{\sqrt{2}}\frac{K_E^\infty}{|K_E^\infty|}\cos\left(\frac{1}{2}\Theta-\phi\right) \quad \text{for } R>R_0. \end{aligned} \tag{12}$$

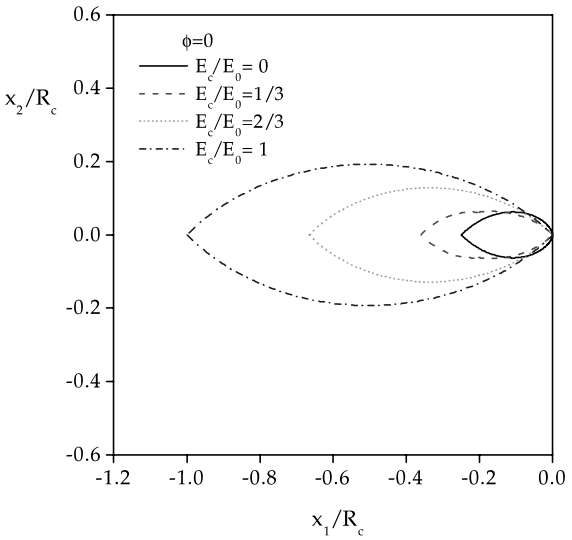

Fig. 3. 90° domain switching zones for $\phi = 0$ with various E_c/E_0.

In the limiting case as $E_0 \to \infty$, (11) and (12) reduce to the following closed form:

$$\sqrt{\frac{R}{R_c}} = \frac{1}{\sqrt{2}} \frac{K_E^\infty}{|K_E^\infty|} \cos\left\{\frac{1}{2}\theta - \left(\phi \pm \frac{3}{4}\pi\right)\right\} \quad \text{for 90°switching,}$$
$$\sqrt{\frac{R}{R_c}} = -\frac{1}{\sqrt{2}} \frac{K_E^\infty}{|K_E^\infty|} \cos\left(\frac{1}{2}\theta - \phi\right) \quad \text{for 180°switching.} \tag{13}$$

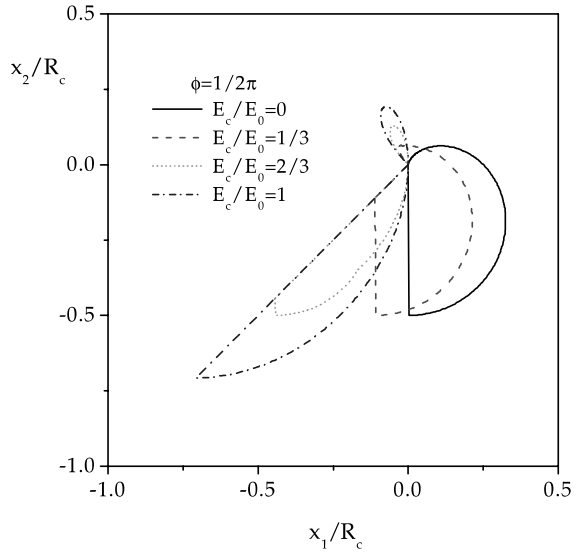

Fig. 4. 90° domain switching zones for $\phi = \frac{1}{2}\pi$ with various E_c/E_0.

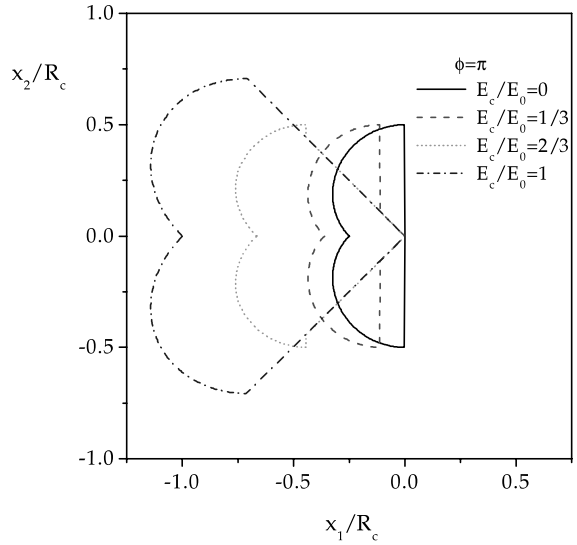

Fig. 5. 90° domain switching zones for $\phi = \pi$ with various E_c/E_0.

The switching zone boundaries inside and outside the electrical nonlinear zone are determined from (11) and (12) so as to satisfy the conditions $0 \leqslant r \leqslant 2R_0 \cos\theta$ and $R \geqslant R_0$, respectively. The domain switching is assumed to occur in the direction with larger value of r or R when the criterion (1) is satisfied for 90° switching and 180° switching. The forms of the 90° switching zone boundaries predicted from (11) and (12) are shown in Figs. 3–5 for $\phi = 0$, $\frac{1}{2}\pi$ and π respectively with four specific values of E_c/E_0. It is seen from Figs. 3–5 that the shape and size of the switching zone depend strongly on the angle of the polarization vector, ϕ and the ratio of the coercive electric field to the yield electric field, E_c/E_0. The switching zone size becomes larger as E_c/E_0 increases. In general, the switching zones are not symmetric about the crack plane except $\phi = 0, \pm\pi$. Non zero crack tip stress intensity factor of the Mode II for the crack due to the domain switching may be occurred.

5. Stress intensity factor

The present section is devoted to the determination of a universal relation between the local crack tip stress intensity factor and the applied intensity factor of electric field under the small scale conditions. We first consider mono-domain ferroelectrics with a uniform poling direction ϕ. The switching strains are a typical example of eigenstrains (Mura, 1987). The switching strains are prohibited from taking place freely because of restrictions placed on the boundary of the switching zone under the constraint of the unswitched material. An additional deformation is thus created within the material both outside and inside switching zone to match the displacements and surface tractions along the boundary of the switching zone. Due to the incompatibility of the strains induced by the domain switching around the crack tip, the eigenstress, which is self-equilibrated internal stresses, are generated. Therefore, the local crack tip stress intensity factors induced by domain switching can be evaluated by an Eshelby technique. According to Rice (1985) and Gao (1989) for an elastic material with transformation strains, the explicit form of crack tip stress intensity factors can be expressed as

$$K_\alpha^{\mathrm{tip}} = \frac{Y}{1+v}\int_A U_{ij}^\alpha \Delta\gamma_{ij}\,\mathrm{d}A(\alpha = \mathrm{I}, \mathrm{II}). \tag{14}$$

Here we are only concerned with the case in which the crack surfaces remain open. $K_{\mathrm{I}}^{\mathrm{tip}}$ and $K_{\mathrm{II}}^{\mathrm{tip}}$ are the Mode I and Mode II crack tip stress intensity factors induced by the switching strains, respectively. Y and v denote the Young's modulus and the Poisson's ratio, respectively. A is the switching region. $U_{ij}^\alpha(r,\theta)(\alpha = \mathrm{I}, \mathrm{II})$ are the near-tip weight functions given by

$$\begin{aligned}
\mathbf{U}^{\mathrm{I}}(r,\theta) &= \frac{1}{16(1-v)\sqrt{2\pi}r^{3/2}}\begin{bmatrix} \cos\frac{3}{2}\theta + 3\cos\frac{7}{2}\theta & -3\sin\frac{3}{2}\theta + 3\sin\frac{7}{2}\theta \\ -3\sin\frac{3}{2}\theta + 3\sin\frac{7}{2}\theta & 7\cos\frac{3}{2}\theta - 3\cos\frac{7}{2}\theta \end{bmatrix}, \\
\mathbf{U}^{\mathrm{II}}(r,\theta) &= \frac{1}{16(1-v)\sqrt{2\pi}r^{3/2}}\begin{bmatrix} -5\sin\frac{3}{2}\theta - 3\sin\frac{7}{2}\theta & \cos\frac{3}{2}\theta + 3\cos\frac{7}{2}\theta \\ \cos\frac{3}{2}\theta + 3\cos\frac{7}{2}\theta & -3\sin\frac{3}{2}\theta + 3\sin\frac{7}{2}\theta \end{bmatrix}.
\end{aligned} \tag{15}$$

Once the boundary of the domain switching zone is determined from (11) and (12), the crack tip stress intensity can be calculated by (14).

Introducing integrals $F_\alpha(\alpha = \mathrm{I}, \mathrm{II})$ defined by

$$F_{\mathrm{I}} = \frac{3}{8\pi}\int_{-\pi}^{\pi}\sqrt{\frac{r}{R_{\mathrm{c}}}}\left[\cos\left(\frac{3}{2}\theta - 2\phi\right) - \cos\left(\frac{7}{2}\theta - 2\phi\right)\right]\mathrm{d}\theta,$$
$$F_{\mathrm{II}} = \frac{3}{8\pi}\int_{-\pi}^{\pi}\sqrt{\frac{r}{R_{\mathrm{c}}}}\left[\sin\left(\frac{3}{2}\theta - 2\phi\right) + 3\sin\left(\frac{7}{2}\theta - 2\phi\right)\right]\mathrm{d}\theta, \tag{16}$$

the expressions of K_α^{tip} $(\alpha = \mathrm{I}, \mathrm{II})$ in (14) are rewritten as

$$K_\alpha^{\mathrm{tip}} = \eta K_{\mathrm{E}}^{\infty} F_\alpha(E_{\mathrm{c}}/E_0; \phi). \tag{17}$$

here r is the boundary of the 90° switching zone as a function of θ and η is the given by

$$\eta = \frac{Y\gamma_{\mathrm{s}}}{(1-\nu^2)E_{\mathrm{c}}}. \tag{18}$$

It is noted that K_α^{tip} depends linearly on K_{E}^{∞} since the integral $F_\alpha(\alpha = \mathrm{I}, \mathrm{II})$ is a function of E_{c}/E_0 and ϕ only. Once the integral in (16) is carried out numerically, K_α^{tip} $(\alpha = \mathrm{I}, \mathrm{II})$ Now, we can be obtained directly. In Figs. 6 and 7, the numerical results of the Mode I and Mode II crack tip stress intensity factors due to the switching are plotted as a function of E_{c}/E_0, for mono-domain ferroelectrics with specific values of ϕ. As observed in Figs. 6 and 7, the variations of K_α^{tip} may exhibit very different aspects. K_α^{tip} depends on E_{c}/E_0 and ϕ strongly. E_{c}/E_0 plays a significant role in determining the sign of $K_{\mathrm{I}}^{\mathrm{tip}}$. $K_{\mathrm{I}}^{\mathrm{tip}}$ is negative at small E_{c}/E_0 and becomes positive under certain values of E_{c}/E_0. The negative stress intensity factor leads to overlapping of the crack surfaces. The surfaces of the crack are thus contact near the crack tip. This result implies that under purely electrical loading, fracture may occur for a ferroelectric material with the value of E_{c}/E_0 near 1 while fracture of a ferroelectric material with a very small E_{c}/E_0 can not be caused for $\phi = 0, \pm\pi$. Fig. 8 shows the crack tip intensity factors as a function of ϕ for the case of $E_{\mathrm{c}}/E_0 = 0.3$. It is noted that $K_{\mathrm{I}}^{\mathrm{tip}}$ is an even function of ϕ and $K_{\mathrm{II}}^{\mathrm{tip}}$ is an odd function of ϕ.

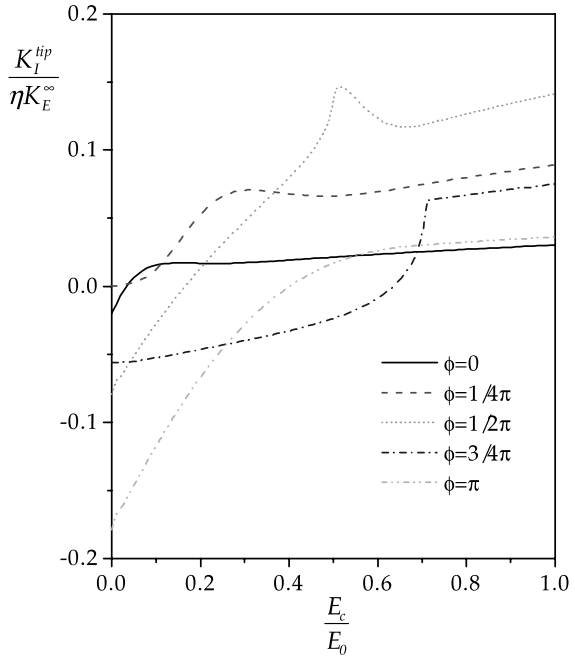

Fig. 6. Mode I crack tip stress intensity factor as a function of E_{c}/E_0 with various ϕ.

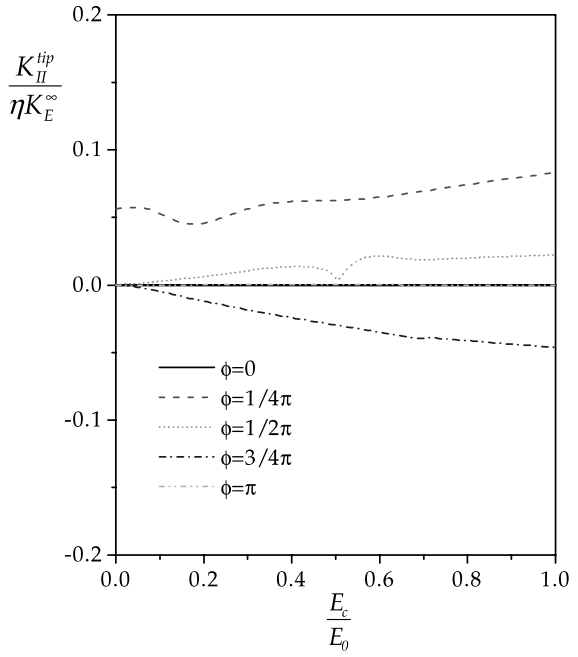

Fig. 7. Mode II crack tip stress intensity factor as a function of E_c/E_0 with various ϕ.

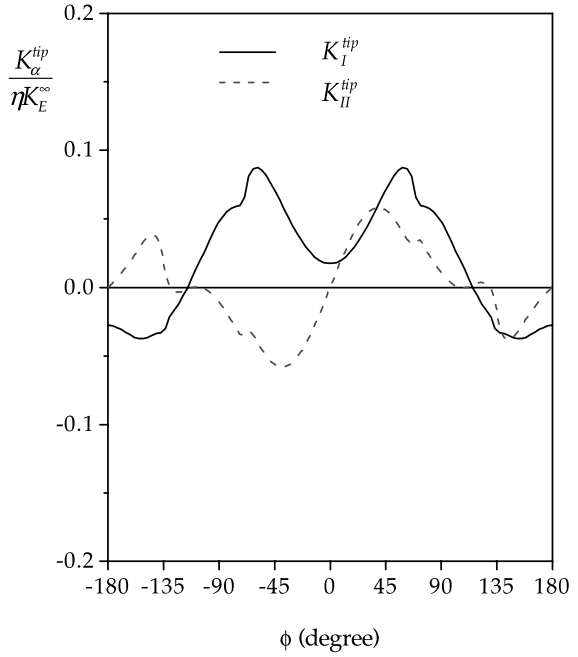

Fig. 8. Crack tip stress intensity factors as a function of ϕ with $E_c/E_0 = 0.3$.

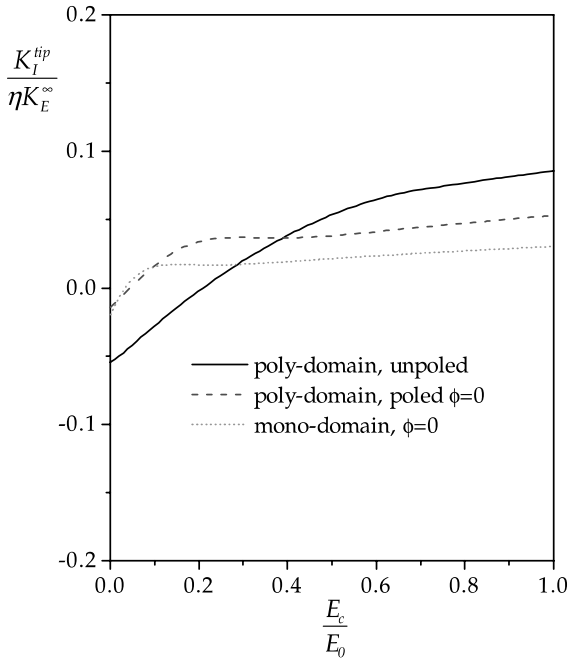

Fig. 9. Crack tip stress intensity factors as a function of E_c/E_0.

Next, we consider poly-domain ferroelectrics. Employing a Reuss type approximation, the crack tip stress intensity factors for fully poled poly-domain ferroelectrics with a poling direction ω can be given as (Yang and Zhu, 1998)

$$K_\alpha^{\text{tip}} = \frac{2}{\pi}\int_{\omega-1/4\pi}^{\omega+1/4\pi} K_\alpha^{\text{tip}}(E_c/E_0;\phi)\,\mathrm{d}\phi. \tag{19}$$

Details for the limitations in using the Reuss type approximation have been presented in Yang and Zhu (1998). In a similar manner, the crack tip stress intensity factors for unpoled poly-domain ferroelectrics can be obtained approximately by

$$K_\alpha^{\text{tip}} = \frac{1}{2\pi}\int_{-\pi}^{\pi} K_\alpha^{\text{tip}}(E_c/E_0;\phi)\,\mathrm{d}\phi. \tag{20}$$

Fig. 9 shows the numerical results of the crack tip stress intensity factors for a fully poled poly-domain material with $\omega = 0$ and a unpoled poly-domain material. The crack tip stress intensity factors for the poly-domain ferroelectrics become larger than those for the mono-domain material with $\phi = 0$ as E_c/E_0 increases. The stress intensity factor of the Mode II for a fully poled poly-domain material with $\omega = 0$ and a unpoled poly-domain material is not induced since $K_{\text{II}}^{\text{tip}}(E_c/E_0;\phi)$ for a mono-domain material is an odd function of ϕ.

6. Electrical fracture toughness

The crack tip stress intensity factor due to the domain switching is obtained numerically for the crack under purely electrical loading as shown in the previous section. We examine the electrical fracture

toughness of unpoled poly-domain ferroelectrics. $K_{\mathrm{I}}^{\mathrm{tip}}$ may be used as a fracture parameter governing the fracture processes near the crack tip. The onset of crack growth occurs when $K_{\mathrm{I}}^{\mathrm{tip}}$ reaches the fracture toughness of the material. The apparent electrical fracture toughness is the critical value of K_{E}^{∞} when fracture occurs. The solution of the crack tip stress intensity factor for the crack in the unpoled poly-domain ferroelectric material can be used to determine the electrical fracture toughness, which results in

$$K_{\mathrm{EC}} = \frac{K_{\mathrm{IC}}}{\eta F_{\mathrm{I}}(E_{\mathrm{c}}/E_0)}. \tag{21}$$

Here K_{IC} and K_{EC} are the mechanical and electrical fracture toughnesses, respectively. $F_{\mathrm{I}}(E_{\mathrm{c}}/E_0)$ is the dimensionless function defined as

$$F_{\mathrm{I}}(E_{\mathrm{c}}/E_0) = \frac{1}{2\pi}\int_{-\pi}^{\pi} F_{\mathrm{I}}(E_{\mathrm{c}}/E_0;\phi)\,\mathrm{d}\phi. \tag{22}$$

It is noted that (21) is valid when $F_{\mathrm{I}}(E_{\mathrm{c}}/E_0)$ has a positive value. Under purely electrical loading, fracture does not occur for a ferroelectric material with a negative F_{I}. Under the purely electrical loading, the critical value of energy release rate, $G_{\mathrm{C}}^{\mathrm{E}}$ is related to the electrical fracture toughness by

$$G_{\mathrm{C}}^{\mathrm{E}} = \frac{1}{2}\varepsilon(K_{\mathrm{EC}})^2. \tag{23}$$

Now, we consider the asymptotic problem of a semi-infinite crack in a ferroelectric ceramic under purely mechanical loading. Tractions vanish on the crack surfaces. The remote stress fields in the asymptotic problem are given by the Mode I near-tip fields for the crack in the linear material. The domain switching induced by the purely mechanical loading makes no contribution to $\Delta K_{\mathrm{I}}^{\mathrm{tip}}$, which has been shown for elastic ceramics with dilatant transformation by McMeeking and Evans (1982) and Budiansky et al. (1983). Thus, we have $K_{\mathrm{I}}^{\mathrm{tip}} = K_{\mathrm{I}}^{\infty}$ for the stationary crack under purely mechanical loading, where K_{I}^{∞} denotes the applied stress intensity factor of the Mode I. Under the purely mechanical loading, the critical value of energy release rate, $G_{\mathrm{C}}^{\mathrm{M}}$ is related to the mechanical fracture toughness by

$$G_{\mathrm{C}}^{\mathrm{M}} = \frac{1-\nu^2}{Y}(K_{\mathrm{IC}})^2. \tag{24}$$

The ratio of the critical electrical energy release rate to the critical mechanical energy release rate is obtained from (21)–(23) as

$$\frac{G_{\mathrm{C}}^{\mathrm{E}}}{G_{\mathrm{C}}^{\mathrm{M}}} = \frac{1}{2}\lambda\frac{1}{\{F_{\mathrm{I}}(E_{\mathrm{c}}/E_0)\}^2}, \tag{25}$$

where λ is the dimensionless parameter as follows:

$$\lambda = \frac{(1-\nu^2)\varepsilon E_{\mathrm{c}}^2}{Y\gamma_{\mathrm{s}}^2}. \tag{26}$$

7. Concluding remarks

Conducting cracks in ferroelectric ceramics under purely electrical loading are analyzed to investigate the effects of electric fields on fracture behavior. In order to derive the relation between the crack tip stress intensity factor and the applied intensity factor of electric field under small scale conditions, the asymptotic problem of a semi-infinite conducting crack in a mono-domain ferroelectric material is considered. The shape of the domain switching zone attending the crack tip in order to evaluate the crack tip stress intensity

factor due to the domain switching is estimated based on the nonlinear domain switching model. It is shown that the switching zone boundary and the crack tip stress intensity factors due to the switching depend strongly on the angle of the polarization vector and the ratio of the coercive electric field to the yield electric field. Especially, it is found that the crack tip stress intensity factor is negative at small value of the ratio of the coercive electric field to the yield electric field. This result implies that under purely electrical loading, fracture of a mono-domain ferroelectric material with a very small value of the ratio of the coercive electric field to the yield electric field may not be caused for the conducting crack parallel to the poling axis. A conducting crack in poly-domain ferroelectrics is also considered. The electrical fracture toughness of poled poly-domain ferroelectrics is examined. Employing a Reuss type approximation, the crack tip stress intensity factors for a fully poly-domain ferroelectric material as well as unpoled poly-domain material are obtained. The ratio of the critical electrical energy release rate to the critical mechanical energy release rate is obtained. The results predicted theoretically here provide a theoretical explanation for the experimental observation on electrical fracture toughness of ferroelectric materials.

References

Beom, H.G., 1999. Small scale nonlinear analysis of electrostrictive crack problems. J. Mech. Phys. Solids 47, 1379–1395.

Beom, H.G., Atluri, S.N., 2003. Effect of electric fields on fracture behavior of ferroelectric ceramics. J. Mech. Phys. Solids 51, 1107–1125.

Budiansky, B., Hutchinson, J.W., Lambropoulos, J.C., 1983. Continuum theory of dilatant transformation toughening ceramics. Int. J. Solids Struct. 19, 337–355.

Fu, R., Qian, C.-F., Zhang, T.-Y., 2000. Electrical fracture toughness for conductive cracks driven by electrical fields in piezoelectric materials. Appl. Phys. Lett. 76, 126–128.

Gao, H., 1989. Application of 3-D weight functions—I. Formulations of crack interfaces with transformation strains and dislocations. J. Mech. Phys. Solids 37, 133–153.

Heyer, V., Schneider, G.A., Balke, H., Drescher, J., Bahr, H.-A., 1998. A fracture criterion for conducting cracks in homogeneously poled piezoelectric PZT-PIC 151 ceramics. Acta Mater. 46, 6615–6622.

Huber, J.E., Fleck, N.A., Landis, C.M., McMeeking, R.M., 1999. A constitutive model for ferroelectric polycrystals. J. Mech. Phys. Solids 47, 1663–1697.

Hwang, S.C., Lynch, C.S., McMeeking, R.M., 1995. Ferroelectric/ferroelastic interactions and a polarization switching model. Acta Metall. Mater. 43, 2073–2084.

McMeeking, R.M., Evans, A.G., 1982. Mechanics of transformation-toughening in brittle materials. J. Am. Ceram. Soc. 65, 242–246.

Mura, T., 1987. Mechanics of Defects in Solids. Martinus Nijhoff, London.

Kamlah, M., Tsakmakis, C., 1999. Phenomenological modeling of the non-linear electro-mechanical coupling in ferroelectrics. Int. J. Solids Struct. 36, 669–695.

Rajapakse, R.K.N.D., Zeng, X., 2001. Toughening of conducting cracks due to domain switching. Acta Mater. 49, 877–885.

Rice, J.R., 1985. Three-dimensional elastic crack tip interactions with transformation strains and dislocations. Int. J. Solids Struct. 21, 781–791.

Ru, C.Q., Mao, M., 1999. Conducting cracks in a piezoelectric ceramic of limited electrical polarization. J. Mech. Phys. Solids 47, 2125–2146.

Suo, Z., 1993. Models for breakdown-resistant dielectric and ferroelectric ceramics. J. Mech. Phys. Solids 41, 1155–1176.

Sze, K.Y., Pan, Y-S., 2001. Nonlinear fracture analysis of piezoelectric ceramics by finite element method. Eng. Fract. Mech. 68, 1335–1351.

Wang, T., Zhang, T.-Y., 2001. Electrical fracture toughness for electrically conductive deep notches driven by electrical fields in depoled lead zirconate titanate ceramics. Appl. Phys. Lett. 79, 4198–4200.

Yang, W., Zhu, T., 1998. Switch-toughening of ferroelectrics under electric field. J. Mech. Phys. Solids 46, 291–311.